*Journal of Thermal Analysis and Calorimetry, Vol. 84 (2006) 2, 497–501*

# PHASE TRANSFORMATION IN SPODUMENE–DIOPSIDE GLASS

*H. Anmin*[*]*, L. Ming and M. Dali*

The State Key Laboratory of the Metal Matrix Composites, Shanghai Jiaotong University, 1954 Huashan road, Shanghai, P. R. China

In situ developments of platelike spodumene–diopside grains were obtained by controlled devitrification of the complex system $Li_2O$–CaO–MgO–$Al_2O_3$–$SiO_2$ glass. The crystallization mechanisms of spodumene–diopside glass were measured by isothermal and non-isothermal processes using classical and differential thermal analysis techniques. The Avrami constant *n* was 2.0–2.1, indicating two-dimensional crystal growth and platelike grains. The crystalline phases precipitated first were high-quartz$_{s.s.}$, then transformed to β-spodumene and diopside. The Flexural strength, fracture toughness and thermal shock resistance (in 20°C water) increased from 145 MPa, 1.3 MPa $m^{1/2}$, 800°C (pure spodumene) to 197 MPa, 2.9 MPa $m^{1/2}$ and 920°C (spodumene–diopside) with low thermal expansion coefficient (from $3\sim9\cdot10^{-7}$ to $11.8\cdot10^{-7}$ $K^{-1}$). This mean in situ developments of platelike spodumene–diopside grains reinforced the low thermal expansion coefficient glass-ceramics.

***Keywords:*** *crystallization, glass ceramic, heat treatment, nucleation*

## Introduction

Lithium aluminumsilicate glass-ceramics ($Li_2O$–$Al_2O_3$–$SiO_2$, LAS) have very low thermal expansion coefficient, transparency, excellent thermal and chemical durability, and have achieved great industrial and economical importance [1–3]. But they have low strength (100 MPa for high-quartz$_{s.s.}$ and 150 MPa for β-spodumene) and high melting temperature. To obtain lower melting temperature, MgO, ZnO, CaO, etc. had been added in LAS glass ceramics to low the melting point, to regulate the thermal expansion coefficient and so on for many years [4–6]. In order to improve mechanical properties, whiskers, fibers and granule were dispersed in the glass ceramics matrix because of that they could promote crack defection and grain bridging. But these methods lead new problem, such as transient stress between the matrixes and disperse phase [7].

Generally, the properties of the glass-ceramics are determined by the main crystallization phases precipitated from the base glasses and their microstructures which depended on composition of the parent glass as well as thermal treatment and addition of nucleating agents. To achieve desired microstructure and properties, it is important to design the composition and control the crystallization of the glass [1–5]. Diopside has high bending strength (300 MPa) and high fracture toughness (3.5 MPa $m^{1/2}$) [5, 6]. Ashizuka has reported that CaO–MgO–$SiO_2$–$P_2O_5$ glass-ceramics with precipites of diopside and apatite had a high strength of 236 MPa [8]. So, by adding CaO and MgO to LAS glass ceramics and controlling $Li_2O$–CaO–MgO–$Al_2O_3$–$SiO_2$ devitrification, spodumene–diopside glass ceramics may obtain. The spodumene ($Li_2O$–$Al_2O_3$–$SiO_2$)–diopside (CaO–MgO–$SiO_2$) glass ceramics may have the advantages – low thermal expansion coefficient, low melting point and high bending strength.

Activation energy and crystallization mechanisms are the most important kinetic parameters in the crystallization of glasses [9–18]. These parameters can be obtained by DTA. Two methods, namely isothermal and non-isothermal methods, are usually applied for differential thermal analysis. In the isothermal method, glass samples are quickly heated up and held at a temperature above the glass transition temperature that means crystallization occurs at a constant temperature. In the non-isothermal method, glass samples are heated up at a fixed heating rate and crystallized during DTA scan.

The intention of this study is to investigate the phase transformation in spodumene–diopside glasses, and in order to evaluate the potential use for the glass-ceramics.

## Experimental

The starting materials were analytical grade reagents (mass%): 61.5$SiO_2$, 14.4$Al_2O_3$, 6.1MgO, 4.0$Li_2O$, 7.0CaO and 7.0$TiO_2$. Glass batches were well mixed by ball-milling for 12 h, and thereafter melted in alumina crucibles at 1500°C in an electric furnace for 2 h. The

* Author for correspondence: huanmin@tsinghua.org.cn

*1388–6150/$20.00*

*Akadémiai Kiadó, Budapest, Hungary*
*Springer, Dordrecht, The Netherlands*

as-cast glass samples were annealed at 600°C for 1 h followed by slow cooling to the room temperature. DTA scans of annealed glass specimens were carried out in a Dupont 2100 Thermal Analyzer. After crushing annealed glasses to the size of about 100–200 mesh, non-isothermal and isothermal experiments were performed by heating 30 mg glass samples in a Pt crucible and using $Al_2O_3$ as the reference material in the temperature ranging from 20 to 1200°C.

The characterization of the glass-ceramic samples was carried out using both X-ray diffraction and electron microscopy techniques (SEM). X-ray diffraction (XRD) investigations were done with a D-max-RB diffractometer with $CuK_\alpha$ radiation ($\chi_{K\alpha 1}$=1.5406 Å) operating at 35 kV and 40 mA in the 2θ range from 10 to 70° at 0.02° steps. SEM was done with a JSM-6301F. Optical mount specimens were prepared with standard metallographic techniques followed by chemical etching in an HF solution (5%) for 1.5 min. Etched glass-ceramic samples were coated with a thin layer of gold.

The strength was measured in ten specimens using a 4-point bending fixture with a span of 30 mm at a crosshead speed of 0.5 mm $min^{-1}$. The fracture toughness was measured by an indentation fracture (IF) method using the Evans equation to calculate $K_{IC}$ from the length of the crack and the semi-diagonal of the indentation [19].

## Results and discussion

*Non-isothermal transformation kinetics*

DTA curves of the glasses at heating rates of 5, 10, 15, 20 K $min^{-1}$ are shown in Fig. 1. Only one exothermal peak appeared in the DTA scan curves [1–3], this exothermal peak was associated with high-quartz$_{s.s.}$ precipitated which could be seen from XRD analysis. As seen in Fig. 1, the crystallization peak temperatures and heights increased with heating rate. Because in quenched samples without nucleation treatment, as in this study, nuclei are formed during DTA scans, it is necessary to have an induction time for nucleation to occur, when the heating rate increases, the time to reach the desired temperature decreases and there is a minor soaking time in the nucleation range. Consequently, crystallization begins at relatively higher temperatures and higher speed. This result is in good agreement with previous reports [20, 21].

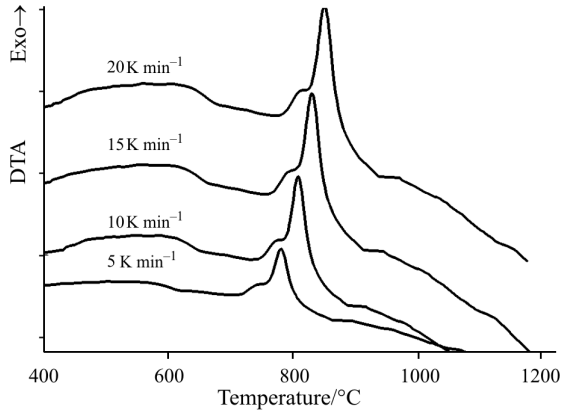


**Fig. 1** DTA plots of the glass at different heating rates

From the Johnson–Mehl–Avrami (JMA) equation [9–12], non-isothermal crystallization kinetics of glass be expressed by Kissinger equation [13–15]:

$$\ln\frac{T_p^2}{\alpha} = \frac{E}{RT_p} + \ln\frac{E}{R\nu} \quad (1)$$

where $T_p$ is the crystallization peak maximum temperature in a DTA curve, α is the heating rate, $R$ is the gas constant and $E$ is activation energy for the phase transformation. Figure 2 shows the plot of $\ln(T_p^2/\alpha$ *vs.* $1000/T_p$. Activation energy $E$ was determined as 369 kJ $mol^{-1}$.

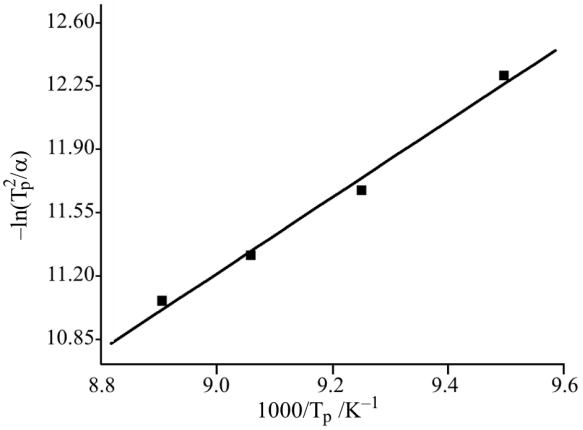


**Fig. 2** The plots of $\ln(T_p^2/\alpha)$ *vs.* $1000/T_p$

The value of the Avrami parameter or the order of the crystallization reaction, $n$, was determined by the Ozawa equation [17]:

$$\ln[-\ln(1-x)]_T = -n\ln\alpha + \text{const} \quad (2)$$

In Eq. (2), $x$ is the volume fraction crystallized at a fixed temperature $T$, α is the DTA scan rate, the plot of $\ln[-\ln(1-x)]$ *vs.* lnα at 760°C is showed in Fig. 3. A value of $n$ determined from the slopes using linear regression analysis is 2.0. The value of $n$ close to 1 means that surface crystallization dominates crystallization while the value of 3 implies a significant contribution of the bulk crystallization process, the Avrami parameters $n$ closed to 2.0 indicate crystallization is between surface crystallization and bulk crystallization in this glass, and this means a plate-like development of the crystallization centers.

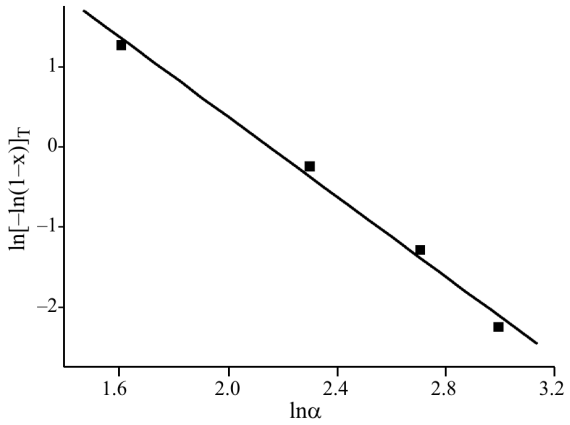


**Fig. 3** The Ozawa plot of $\ln[(-\ln(1-x))]_T$ *vs.* lnα for determination of *n*

From the values of activation energy, the Avrami parameters (*n*) are calculated by the Augis–Bennett equation [18]:

$$n = \frac{2.5}{\Delta T}\frac{RT_p^2}{E} \quad (3)$$

In Eq. (3), $\Delta T$ is the full width of the exothermic peak at the half maximum intensity. As can see from the calculation, the value of *n* is 2.1. It showed good agreement with Ozawa method [15].

*Isothermal transformation kinetics*

The glass power was isothermally heated at 750, 760, 770 and 780°C. The typical isothermal DTA curve (760°C) is showed in Fig. 4. The isothermal devitrification kinetics of glass are described by the Johnson–Mehl–Avrami (JMA) equation [9–11].

$$x = 1 - \exp[-(kt)]^n \quad (4)$$

In Eq. (4), *x* is the volume fraction crystallized at a given temperature during time *t*; *n* is the Avrami exponent, which is dependent on the crystallization mechanism; and *k* is the crystallization rate constant, which is usually assigned an Arrhenian temperature dependence:

$$k = \nu \exp\left(-\frac{E}{RT}\right) \quad (5)$$

In Eq. (5), ν is the frequency factor, *R* is the gas constant, *T* is the absolute temperature, and *E* is the effective overall activation energy. Taking natural logarithm for both Eqs (4) and (5), the equations can be as follows:

$$\ln[-\ln(1-x)]_T = n\ln k + n\ln t \quad (6)$$

and

$$\ln k = \ln\nu - \frac{E}{RT} \quad (7)$$

According to the Eq. (6), Fig. 5 showed the plot of $\ln[-\ln(1-x)]$ *vs.* ln*t* at different temperatures from 750 to 780°C. The Avrami exponents *n* are the slope of the curves, which are 1.94, 2.02, 2.11, 2.17, and *n*ln*k* can be obtained by the intercept, so ln*k* are obtained.

From the Eq. (7), by plotting ln*k* *vs.* 1/*T*, as shown in Fig. 6, the activation energy is 392 kJ mol$^{-1}$.

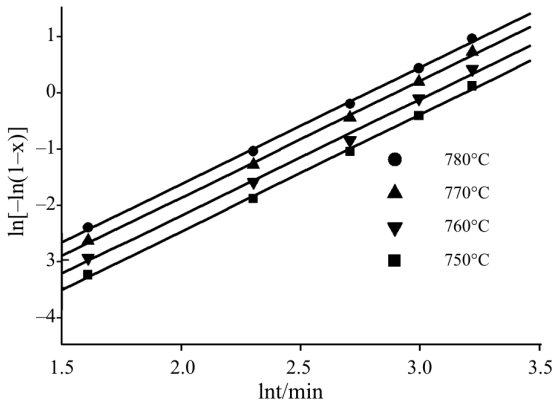


**Fig. 5** The plots of $\ln[-\ln(1-x)]$ *vs.* ln*t* for *n* and ln*k*

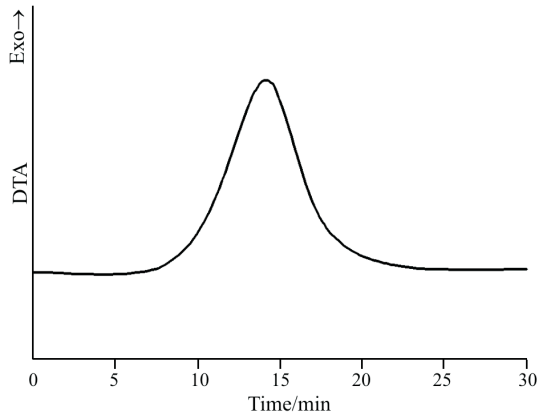


**Fig. 4** A typical DTA curve of LCMAS glass power isothermally heated at 760°C

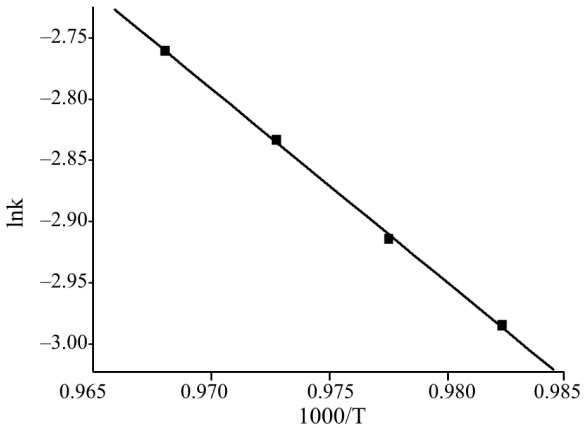


**Fig. 6** Arrhenian plot of ln*k* *vs.* 1000/*T* for *E*

As in glass transformation procedure, Si–O and Al–O bands break, the dissociation energy for Si–O bonds is 445 kJ $mol^{-1}$ and for Al–O bonds is 330–423 kJ $mol^{-1}$. Thus the activation energy for transformation (369–392 kJ $mol^{-1}$) is lower than the dissociation energy values for the ion bonds. It is reasonable to think that during the crystallization procedure, the strengths of Li–O, Ca–O, Mg–O bonds, which is 326, 331 and 287 kJ $mol^{-1}$ [22], should be considered. As the presence of nucleating agents ($TiO_2$), phase separation occurred on cooling from the melting, and subsequent heating caused the formation of a large number of little aluminium titanate crystals. These crystals acted as sites for heterogeneous nucleation. Therefore, it is obviously that various combinations could take place simultaneously.

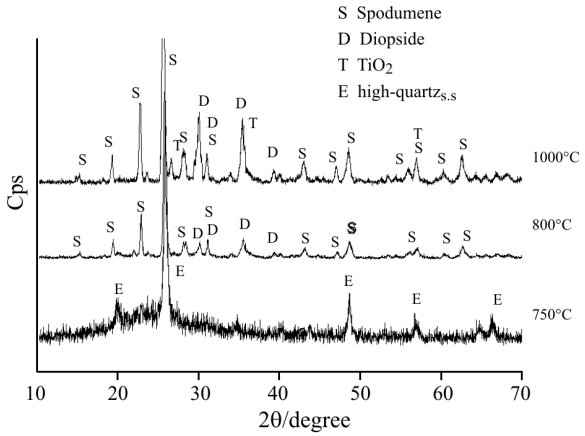


**Fig. 7** XRD patterns of glass samples after heat treated at 750, 850 and 1000°C for 2 h

*X-ray diffraction (XRD)*

Figure 7 illustrates the powder XRD results of glasses crystallized at 750, 850, 1000°C for 2 h. As crystallized at 750°C, a broadening scattering intensity associated with residual glass phase was observed for the samples and small high-$quartz_{s.s.}$ appeared. After being heated at 850°C, high-$quartz_{s.s.}$ transformed to β-spodumene and diopside appeared, the main crystalline was β-spodumene and minor phase was diopside. When the temperature increased to 1000°C, the amount of β-spodumene and diopside increased, and minor $TiO_2$ phase appear.

*Microstructure and mechanical properties*

Figure 8 shows the microstructure of the glass heat treated at 750, 1000°C for 2 h. After crystallized at 750°C, the sample showed little crystal in glass matrix, according to XRD result, this crystal is high-$quartz_{s.s.}$. As the heating temperature increased to 1000°C, the grain showed a platelike morphology. This platelike morphology indicates that crystallization mechanism is surface crystallization to bulk crystallization in this glass, and the Avrami parameter *n* is closed to 2 [4, 6].

The mechanical properties of spodumene and spodumene–diopside glass ceramics after crystallized at 1000°C/2 h are shown in Table 1. It is clear that spodumene–diopside glass ceramics have great advantage on flexural strength, fracture toughness and thermal shock resistance, in spite of some higher thermal expansion coefficient than that of spodumene glass ceramics. The increasing of mechanical proper-

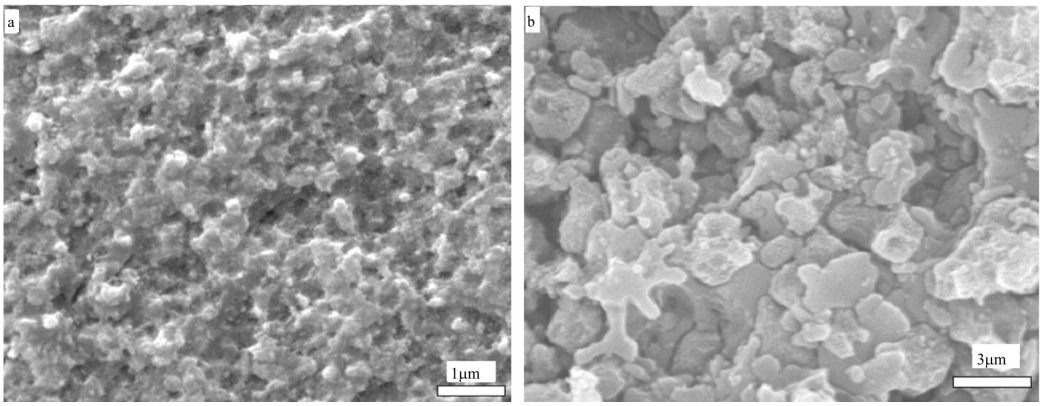


**Fig. 8** SEM pictures showing the microstructure of the glass crystallized at a – 750 and b – 1000°C for 2 h

**Table 1** The mechanical properties of glass-ceramics after crystallized at 1000°C/2 h

| Sample | Thermal expansion coefficient/ $K^{-1}$ | Flextural strength/ MPa | Fracture toughness/ MPa $m^{1/2}$ | Thermal shock resistance/ in 20°C water |
|---|---|---|---|---|
| Spodumene–diopside | $11.8 \cdot 10^{-7}$ | 197 | 2.9 | 920°C |
| Spodumene | $3 \sim 9 \cdot 10^{-7}$ | 145 | 1.3 | 800°C |

ties may be ascribed to the randomly oriented and interlocked spodumene- diopside crystallites, which cause crack, divert or blunt to limit the further development of the flaw size and increase the surface energy of fracture [4–7].

## Conclusions

The phase transformation in spodumene–diopside glass was investigated by isothermal and non-isothermal analysis. The Avrami constant $n$ was 2.0–2.1, indicating two-dimensional crystal growth and platelike grains. The activation energy $E$ was 389–402 kJ $mol^{-1}$, which is lower than that of the diffusion of silicon and aluminum ions. The crystalline phases precipitated first were high-$quartz_{s.s}$, then transformed to β-spodumene and diopside. The flexural strength, fracture toughness and thermal shock resistance (in 20°C water) increased from 145 MPa, 1.3 MPa $m^{1/2}$, 800°C (pure spodumene) to 197 MPa, 2.9 MPa $m^{1/2}$ and 920°C (spodumene–diopside) with low thermal expansion coefficient ($11.8 \cdot 10^{-7}$ $K^{-1}$). This means in situ developments of platelike spodumene–diopside grains reinforced the low thermal expansion coefficient glass-ceramics.

## References


1 P. Riello, P. Canto, N. Comelato, S. Polizzi, M. Verita, G. Fagherazzi, H. Hofmeister and S. Hopfe, J. Non-Cryst. Solids, 288 (2001) 127.
2 L. Barbieri, C. Leonelli, T. Manfredini, C. Siligardi and A. B. Corradi, J. Am. Ceram. Soc., 80 (1997) 3077.
3 L. Arnault, M. Gerland and A. Riviere, J. Mater. Sci., 35 (2000) 2331.
4 H. Scheidler and E. Rodek, Ceram. Bull., 68 (1989) 1926.
5 A. W. A. Elshennawi, E. M. A. Hamzawy, G. A. Khater and A. A. Omar, Ceram. Inter., 27 (2001) 725.
6 R. Cio, P. Pernice, A. Aronne and G. Quattroni, J. Mater. Sci., 28 (1993) 6591.
7 Y. Q. Wu, Y. F. Zhang, X. X. Huang and J. K. Guo, J. Eur. Ceram. Soc., 21 (2001) 581.
8 L. Arnault, M. Gerland and A. Riviere, J. Mater. Sci., 35 (2000) 2331.
9 M. Avrami, J. Chem. Phys., 7 (1939), 1103, 9, 177.
10 W. A. Johnson and K. F. Mehl, Trans. AIME., 135 (1939), pp. 416–442.
11 H. E. Kissinger, J. Res. Nat. Bureau Stand., 57 (1956) 217.
12 I. Waclawska and M. Szumera, J. Therm. Anal. Cal., 72 (2003) 1065.
13 M. Ciecinska, J. Therm. Anal. Cal., 72 (2003) 199.
14 L. Stoch, J. Therm. Anal. Cal., 77 (2004) 7.
15 J. Malek, J. Therm. Anal. Cal., 56 (1999) 763.
16 A. M. Hu, K. M. Liang and F. Peng, Thermochim. Acta, 413 (2004) 53.
17 T. Ozawa, J. Thermal Anal., 31 (1986) 547.
18 J. A. Augis and J. E. Bennett, J. Thermal Anal., 13 (1978) 283.
19 Y. M. Sung, J. Mater. Sci., 37 (2002) 699.
20 C. Păcurariu, M. Liþă, I. Lazău, D. Tiþa and G. Kovacs, J. Therm. Anal. Cal., 72 (2003) 811.
21 J. A. Griggs, K. J. Anusavice and J. J. Mecholsky, Jr., J. Mater. Sci., 37 (2002) 2017.
22 J. M. Rincon, M. Romero, J. Marco and V. Caballer, Mater. Res. Bull., 33 (1998) 1159.


Received: February 16, 2005
Accepted: February 17, 2006

DOI: 10.1007/s10973-005-6941-z